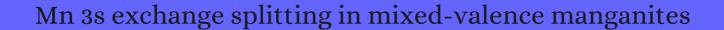
# CITATION REPORT List of articles citing



DOI: 10.1103/physrevb.65.113102 Physical Review B, 2002, 65, .

Source: https://exaly.com/paper-pdf/34129471/citation-report.pdf

Version: 2024-04-23

This report has been generated based on the citations recorded by exaly.com for the above article. For the latest version of this publication list, visit the link given above.

The third column is the impact factor (IF) of the journal, and the fourth column is the number of citations of the article.

#	Paper	IF	Citations
453	Doped manganites beyond conventional double-exchange model. <b>2002</b> , 322, 371-389		14
452	Electronic structure of cobalt-doped manganites. <b>2003</b> , 532-535, 488-492		5
451	Electronic structure of La0.7Sr0.3MnO3 thin films for hybrid organic/inorganic spintronics applications. <b>2003</b> , 94, 7292-7296		84
450	Electronic structure of the transition-metal dicyanamides M[N(CN)2]2 (M=Mn,Fe,Co,Ni,Cu). <i>Physical Review B</i> , <b>2004</b> , 69,	3.3	10
449	Chemical effects in the manganese 3s- <b>3</b> p x-ray emission that follows resonant and nonresonant photon production of a 2p hole. <i>Physical Review B</i> , <b>2004</b> , 70,	3.3	9
448	Initial stages of Mn adsorption on Ge(111). <i>Physical Review B</i> , <b>2004</b> , 70,	3.3	52
447	Electronic and magnetic properties of highly ordered Sr2FeMoO6. <b>2004</b> , 201, 3252-3256		53
446	Valence state of Mn in charge-ordering Pr0.5Ca0.5MnO3lstudied by Mn 3s photoemission spectroscopy. <b>2004</b> , 137-140, 747-750		3
445	Direct observation of high-temperature polaronic behavior in colossal magnetoresistive manganites. <b>2004</b> , 92, 166401		72
444	New redox deposition-precipitation method for preparation of supported manganese oxide catalysts. <b>2005</b> , 101, 151-157		35
443	Evidence for Mn2+ ions at surfaces of La0.7Sr0.3MnO3 thin films. <i>Physical Review B</i> , <b>2005</b> , 71,	3.3	85
442	Core-level spectroscopic study of FeO and FeS2. <i>Physical Review B</i> , <b>2005</b> , 71,	3.3	38
441	A new approach to grafting a monolayer of oriented Mn12 nanomagnets on silicon. <b>2005</b> , 2020-2		71
440	Electronic structure of A- and B-site doped lanthanum manganites: a combined X-ray spectroscopic study. <b>2005</b> , 109, 9354-61		24
439	XPS investigation of Mn valence in lanthanum manganite thin films under variation of oxygen content. <i>Physical Review B</i> , <b>2006</b> , 73,	3.3	293
438	OBound small polarons in oxide materials. <b>2006</b> , 18, R667-R704		145
437	Surface characterization of colossal magnetoresistive manganites La1⊠SrxMnO3 using photoelectron spectroscopy. <b>2006</b> , 153, 37-57		11

436	Semiconductor-metal transition in defect lithium cobaltite. <b>2006</b> , 48, 548-556	27
435	Experimental evidence of the electronic transitions responsible for magneto-optical activity of La1\(\mathbb{R}\)SrxMnO3 (x?0.25). Journal of Magnetism and Magnetic Materials, <b>2006</b> , 300, e126-e129	6
434	Density control of dodecamanganese clusters anchored on silicon(100). <b>2006</b> , 12, 3558-66	25
433	Electronic structure of MnSi: The role of electron-electron interactions. <i>Physical Review B</i> , <b>2006</b> , 73, 3.3	26
432	Structural and magnetic properties of epitaxial thin films of the ordered double perovskite La2CoMnO6. <b>2006</b> , 89, 262503	66
431	Bulk electronic properties of the bilayered manganite La1.2Sr1.8Mn2O7 from hard-x-ray photoemission. <i>Physical Review B</i> , <b>2007</b> , 75,	14
430	Synthesis and Characterization of AgHollandite Nanofibers and Its Catalytic Application in Ethanol Oxidation. <b>2007</b> , 19, 4292-4299	90
429	Electronic structure of a Mn12 molecular magnet: Theory and experiment. <i>Physical Review B</i> , <b>2007</b> , 75,	41
428	Oxygen vacancies and induced changes in the electronic and magnetic structures of La0.66Sr0.33MnO3: A combined ab initio and photoemission study. <i>Physical Review B</i> , <b>2007</b> , 75,	74
427	Catalytic combustion of toluene over mixed CuMn oxides. 2007, 119, 321-326	78
426	Synthesis, characterization, and catalytic application of titanium@ryptomelane nanorods/fibers. <b>2007</b> , 103, 250-256	29
425	Mn-containing catalytic materials for the total combustion of toluene: The role of Mn localisation in the structure of LDH precursor. <b>2007</b> , 119, 327-331	89
424	X-ray spectroscopy of lanthanum manganites: Nature of doping holes, correlation effects, and orbital ordering. <b>2008</b> , 49, 54-58	12
423	Synthesis, characterization, and catalytic activity of cryptomelane nanomaterials produced with industrial manganese sulfate. <b>2008</b> , 327, 393-402	14
422	Hard X-ray PhotoEmission Spectroscopy of strongly correlated systems. <b>2008</b> , 9, 524-536	14
421	Physical properties of La1⊠PbxMnO3 perovskites. <b>2008</b> , 403, 1601-1602	5
420	Facile synthesis of AgDMS-2 nanorods and their catalytic applications in CO oxidation. <b>2008</b> , 116, 586-592	54
419	MnOx-SnO2 Catalysts Synthesized by a Redox Coprecipitation Method for Selective Catalytic Reduction of NO by NH3. <b>2008</b> , 29, 531-536	26

418	Temperature-dependent evolution of the electronic and local atomic structure in the cubic colossal magnetoresistive manganite La1\( \text{La1}\( \text{SrxMnO3}. \) Physical Review B, <b>2008</b> , 77,	3.3	32
417	Surface electronic and magnetic properties of La2/3Sr1/3MnO3 thin films with extended metallicity above the Curie temperature. <i>Physical Review B</i> , <b>2008</b> , 78,	3.3	17
416	Magnetic and dielectric properties of YbMnO3 perovskite thin films. <i>Physical Review B</i> , <b>2008</b> , 78,	3.3	21
415	Defect-induced photoconductivity in layered manganese oxides: a density functional theory study. <b>2008</b> , 100, 146601		84
414	Disproportionation and electronic phase separation in parent manganite LaMnO3. <i>Physical Review B</i> , <b>2009</b> , 79,	3.3	33
413	Further Reading. <b>2009</b> , 17, 113-197		
412	Electronic structures and Hall effect in low-doped La0.9Hf0.1MnO3 epitaxial films. 2009, 105, 07E514		17
411	X-ray photoelectron spectroscopy study of the electronic structure of La1☑ Ca x MnO3+ြsolid solutions. <b>2009</b> , 76, 394-401		10
410	Synthesis and Characterization of Manganese Oxide Catalysts for the Total Oxidation of Ethyl Acetate. <b>2009</b> , 52, 470-481		75
409	X-ray spectroscopic techniques are powerful tools for electronic structure investigations of transition metal oxides. <b>2009</b> , 603, 1613-1621		3
408	Tunnel structure effect of manganese oxides in complete oxidation of formaldehyde. <b>2009</b> , 122, 270-274	4	109
407	Ferromagnetism in epitaxial orthorhombic YMnO3 thin films. <i>Journal of Magnetism and Magnetic Materials</i> , <b>2009</b> , 321, 1719-1722	2.8	34
406	Catalytic oxidation of ethyl acetate over a cesium modified cryptomelane catalyst. 2009, 88, 550-556		53
405	Catalytic performance of manganese cobalt oxides on methane combustion at low temperature. <b>2009</b> , 90, 307-312		149
404	Methyl ethyl ketone combustion over La-transition metal (Cr, Co, Ni, Mn) perovskites. <b>2009</b> , 92, 445-453		45
403	Ferromagnetism and increased ionicity in epitaxially grown TbMnO3 films. <i>Physical Review B</i> , <b>2009</b> , 79,	3.3	52
402	Orientation of Mn12 molecular nanomagnets in self-assembled monolayers. <b>2009</b> , 11, 2192		9
401	Microstructures, surface properties, and topotactic transitions of manganite nanorods. <b>2009</b> , 48, 6242-50	0	49

## (2011-2009)

400	Synthesis, Structure, and Valency Verification of a Mn6IIIO2-Cluster. <b>2009</b> , 223, 145-156		2
399	Carbon Monoxide Oxidation Catalysed by Exotemplated Manganese Oxides. <b>2010</b> , 134, 217-227		56
398	The role of lattice oxygen on the activity of manganese oxides towards the oxidation of volatile organic compounds. <b>2010</b> , 99, 353-363		457
397	Stability of a cryptomelane catalyst in the oxidation of toluene. <b>2010</b> , 154, 308-311		21
396	Charge state of manganese ions and the nonstoichiometry of Ca1 lk La y MnO3 lbingle crystals. <b>2010</b> , 91, 129-133		8
395	Interface properties of magnetic tunnel junction La0.7Sr0.3MnO3/SrTiO3 superlattices studied by standing-wave excited photoemission spectroscopy. <i>Physical Review B</i> , <b>2010</b> , 82,	3.3	69
394	Application of 3s X-Ray Photoelectron Spectra for Determination of Charge States and Magnetic Moments of 3d Ions in Oxides. <b>2010</b> , 168-169, 453-456		1
393	Structure and the Metal Support Interaction of the Au/Mn Oxide Catalysts. <b>2010</b> , 22, 3952-3960		55
392	Characterization of The Lithium Manganese Ferrite LiFeMnO4 Prepared by Two Different Methods. <i>Journal of Physical Chemistry C</i> , <b>2010</b> , 114, 12792-12799	3.8	6
391	Surface complexation of Pb(II) by hexagonal birnessite nanoparticles. <b>2010</b> , 74, 6731-6740		55
390	Significant enhancement of catalytic activities of manganese oxide octahedral molecular sieve by marginal amount of doping vanadium. <b>2010</b> , 11, 871-875		67
389	Synthesis and Properties of Layered-Structured Mn5O8 Nanorods. <i>Journal of Physical Chemistry C</i> , <b>2010</b> , 114, 922-928	3.8	74
388	Valence Band Structure and X-ray Spectra of Oxygen-Deficient Ferrites SrFeOx. <i>Journal of Physical Chemistry C</i> , <b>2010</b> , 114, 5154-5159	3.8	51
387	Structure, dielectric, and magnetic properties of Sr2TiMnO6 ceramics. <b>2010</b> , 108, 094108		30
386	Mn valence, magnetic, and electrical properties of LaMnO3+Ihanofibers by electrospinning. <b>2010</b> , 2, 2689-93		21
385	Tailoring (bio)chemical activity of semiconducting nanoparticles: critical role of deposition and aggregation. <i>Journal of the American Chemical Society</i> , <b>2011</b> , 133, 9536-44	16.4	10
384	Electronic structure of an antiferromagnetic metal: CaCrO3. <i>Physical Review B</i> , <b>2011</b> , 83,	3.3	22
383	Mn Valence Determination for Lanthanum Strontium Manganite Solid Oxide Fuel Cell Cathodes. <b>2011</b> , 158, B1276		16

382	Effects of processing parameters on the properties of lanthanum manganite. 2011, 129, 15-18		4
381	Effect of nanosize on catalytic properties of ferric (hydr)oxides in water: Mechanistic insights. <b>2011</b> , 282, 25-34		27
380	Valence and magnetic state of transition-metal and rare-earth ions in single-crystal multiferroics RMn2O5 (R=Y, Bi, Eu, Gd) from X-ray photoelectron spectroscopy data. <b>2011</b> , 184, 508-516		35
379	Low-temperature selective catalytic reduction of NOx with NH3 over metal oxide and zeolite catalysts review. <b>2011</b> , 175, 147-156		699
378	Chemical Vapor Synthesis and Characterization of Manganese Oxides. <b>2011</b> , 17, 228-234		15
377	Effects of hole doping in electronic states of La1\(\mathbb{R}\)SrxMnO3 probed by magnetic Compton scattering. <b>2011</b> , 98, 052107		8
376	Mn3O4 Supported on Glassy Carbon: An Active Non-Precious Metal Catalyst for the Oxygen Reduction Reaction. <b>2012</b> , 2, 2687-2694		165
375	Physical properties of La1NPbxMnO3 perovskites with 0.24ND.40. <i>Journal of Alloys and Compounds</i> , <b>2012</b> , 535, 129-137	5.7	3
374	Structural and chemical disorder of cryptomelane promoted by alkali doping: Influence on catalytic properties. <b>2012</b> , 293, 165-174		129
373	Valence state of the manganese ions in mixed-valence La1⊞BiMn1+D3⊞Geramics by Mn 2p and Mn 3s X-ray photoelectron spectra. <b>2012</b> , 185, 175-183		41
372	Evidence of electronic band redistribution in La0.65Sr0.35MnO3lby hard x-ray photoelectron spectroscopy. <i>Physical Review B</i> , <b>2012</b> , 86,	3.3	23
371	An analysis of the first steps of phenol adsorption-oxidation over coprecipitated Mn <b>T</b> e catalysts: a DRIFTS study. <b>2012</b> , 107, 295-309		17
370	Electronic properties of embedded MnAs nano-clusters in a GaAs matrix and (Ga,Mn)As films: Evidence of distinct metallic character. <b>2012</b> , 100, 203121		7
369	Interface and Surface Cation Stoichiometry Modified by Oxygen Vacancies in Epitaxial Manganite Films. <b>2012</b> , 22, 4312-4321		54
368	Cu-modified cryptomelane oxide as active catalyst for CO oxidation reactions. <b>2012</b> , 123-124, 27-35		84
367	Nanostructured MnOx as highly active catalyst for CO oxidation. <b>2012</b> , 287, 30-36		70
366	Magnetic properties and magnetocaloric effect in La1.4☑ Ce x Ca1.6Mn2O7 perovskites synthesized by solḡel method. <b>2012</b> , 47, 3125-3130		23
365	Nickel foam supported mesoporous MnO2 nanosheet arrays with superior lithium storage performance. <b>2013</b> , 49, 8459-61		94

## (2013-2013)

364	Controlled synthesis of nanostructured manganese oxide: crystalline evolution and catalytic activities. <b>2013</b> , 15, 7010		130
363	Resistive Switching in Ferromagnetic $frm La_{2/3}$ Resistive		5
362	Single-crystal rare earths manganites La1⊠BixAyMn⊕O3⊞[(A = Ba, Pb): Crystal structure, composition, and Mn ions valence state. X-ray diffraction and XPS study. <b>2013</b> , 186, 14-24		32
361	Transition metal doped cryptomelane-type manganese oxide for low-temperature catalytic combustion of dimethyl ether. <i>Chemical Engineering Journal</i> , <b>2013</b> , 220, 320-327	1.7	108
360	Hard X-ray photoemission with angular resolution and standing-wave excitation. 2013, 190, 165-179		34
359	Determination of electronic and atomic properties of surface, bulk and buried interfaces: Simultaneous combination of hard X-ray photoelectron spectroscopy and X-ray diffraction. <b>2013</b> , 190, 205-209		8
358	Crystal asymmetry and low-angle grain boundary governed persistent photoinduced magnetization in small bandwidth manganites. <b>2013</b> , 113, 063906		14
357	Porous calciumhanganese oxide microspheres for electrocatalytic oxygen reduction with high activity. <b>2013</b> , 4, 368-376		147
356	Precursor-based methods for low-temperature synthesis of defectless NaMnPO4 with an olivine- and maricite-type structure. <b>2013</b> , 15, 9080		33
355	State of manganese atoms in the Nd1+x Sr2⊠ Mn2O7l₃olid solution. <b>2013</b> , 39, 73-76		1
354	Phase, morphology and core-level electron spectroscopy of nano-sized La0.65Sr0.35MnO3 powders prepared by solution combustion synthesis. <b>2013</b> , 74, 315-321		19
353	Effects of substitution of Pr, Nd, and Sm for La on the magnetic properties and magnetocaloric effect of La1.4Ca1.6Mn2O7. <i>Journal of Alloys and Compounds</i> , <b>2013</b> , 553, 129-134	7	16
352	Spectroscopic characterization of MnIIoIIe mixed oxides, active catalysts for COPROX reaction. <b>2013</b> , 38, 5645-5654		40
351	Effect of surface decoration with LaSrFeO4 on oxygen mobility and catalytic activity of La0.4Sr0.6FeO3In high-temperature N2O decomposition, methane combustion and ammonia oxidation. <b>2013</b> , 457, 42-51		39
350	Influence of silver on the catalytic properties of the cryptomelane and Ag-hollandite types manganese oxides OMS-2 in the low-temperature CO oxidation. <b>2013</b> , 462-463, 64-74		88
349	Magnetic and electric properties of CaMn7O12 based multiferroic compounds: effect of electron doping. <b>2013</b> , 25, 246001		19
348	X-ray photoelectron spectroscopy investigation of perovskites La1₪ Sr x FeO3₪ (0 ₪ 2013, 62, 1564-1569		3
347	Analysis of electronic structure and its effect on magnetic properties in (001) and (110) oriented La0.7Sr0.3MnO3 thin films. <b>2013</b> , 25, 376003		10

346	Competition of spin states in heterogenous LaMnO3+□ <b>2014</b> , 53, 123002	1
345	Higher Oxidation State Responsible for Ozone Decomposition at Room Temperature over Manganese and Cobalt Oxides: Effect of Calcination Temperature. <b>2014</b> , 36, 502-512	38
344	Correlation between the electronic and atomic structure, transport properties, and oxygen vacancies on La0.7Ca0.3MnO3 thin films. <b>2014</b> , 104, 021604	7
343	Enlarged Mn 3s splitting and room-temperature ferromagnetism in epitaxially grown oxygen doped Mn2N0.86 films. <b>2014</b> , 116, 173911	14
342	Clear microstructure-performance relationships in Mn-containing perovskite and hexaaluminate compounds prepared by activated reactive synthesis. <b>2014</b> , 16, 4050-60	25
341	Mixed-valence La0.80(Ag1⊠ Sr x )0.20MnO3 manganites with magnetocaloric effect. <b>2014</b> , 49, 633-641	12
340	The Mn(2+)/Mn(3+) state of La0.7Ce0.3MnO3 by oxygen reduction and photodoping. <b>2014</b> , 26, 045502	3
339	Highly selective direct amination of primary alcohols over a Pd/K-OMS-2 catalyst. <b>2014</b> , 309, 439-452	71
338	Sodium deficient nickelthanganese oxides as intercalation electrodes in lithium ion batteries. <i>Journal of Materials Chemistry A</i> , <b>2014</b> , 2, 19383-19395	27
337	Mn2+ cation-directed ionothermal synthesis of an open-framework fluorinated aluminium phosphitephosphate. <b>2014</b> , 4, 29310	4
336	Effect of morphology and manganese valence on the voltage fade and capacity retention of Li[Li2/12Ni3/12Mn7/12]O2. <b>2014</b> , 6, 18868-77	71
335	Characterization and reactivity of biogenic manganese oxides for ciprofloxacin oxidation. <b>2014</b> , 26, 1154-61	45
334	Efficient aerobic oxidation of 5-hydroxymethylfurfural to 2,5-diformylfuran on manganese oxide catalysts. <b>2014</b> , 316, 57-66	108
333	Metal-Organic Chemical Vapor Deposition (MOCVD) Synthesis of Heteroepitaxial Pr0.7Ca0.3MnO3 Films: Effects of Processing Conditions on Structural/Morphological and Functional Properties. <b>2015</b> , 4, 523-32	7
332	Electronic and magnetic properties of epitaxial perovskite SrCrO(0 0 1). 2015, 27, 245605	8
331	Limited nanospace for growth of NiMn composite oxide nanocrystals with enhanced catalytic activity for deep oxidation of benzene. <b>2015</b> , 258, 148-155	22
330	Transition-Metal Phthalocyanines on Transition-Metal Oxides: Iron and Cobalt Phthalocyanine on Epitaxial MnO and TiOx Films. <i>Journal of Physical Chemistry C</i> , <b>2015</b> , 119, 27569-27579	12
329	Post plasma-catalysis for total oxidation of trichloroethylene over CeMn based oxides synthesized by a modified Eedox-precipitation route <b>2015</b> , 172-173, 65-72	63

## (2016-2015)

328	Fermi level shifting, charge transfer and induced magnetic coupling at La0.7Ca0.3MnO3/LaNiO3 interface. <b>2015</b> , 5, 8460		48
327	Electronic structure at transition metal phthalocyanine-transition metal oxide interfaces: Cobalt phthalocyanine on epitaxial MnO films. <b>2015</b> , 142, 101918		14
326	Surface Control of Epitaxial Manganite Films via Oxygen Pressure. <b>2015</b> , 9, 4316-27		26
325	Influence of alkylphosphonic acid grafting on the electronic and magnetic properties of La2/3Sr1/3MnO3 surfaces. <i>Applied Surface Science</i> , <b>2015</b> , 353, 24-28	.7	9
324	Electrochemical Characterization and Quantified Surface Termination Obtained by Low Energy Ion Scattering and X-ray Photoelectron Spectroscopy of Orthorhombic and Rhombohedral LaMnO3 Powders. <i>Journal of Physical Chemistry C</i> , <b>2015</b> , 119, 12209-12217	.8	31
323	Valence state of manganese and iron ions in La1NAxMnO3 (A = Ca, Sr) and Bi1NSrxFeO3 systems from Mn2p, Mn3s, Fe2p and Fe3s X-ray photoelectron spectra. Effect of delocalization on Fe3s 5 spectra splitting. <i>Journal of Alloys and Compounds</i> , <b>2015</b> , 647, 947-955	·7	26
322	Ferroelectric capped magnetization in multiferroic PZT/LSMO tunnel junctions. <b>2015</b> , 106, 132901		8
321	Magnetic properties and magnetocaloric effect in La0.7Sr0.3⊠BixMnO3 manganites. <i>Journal of Alloys and Compounds</i> , <b>2015</b> , 640, 433-439	·7	16
320	Nature of Activated Manganese Oxide for Oxygen Evolution. <i>Journal of the American Chemical Society</i> , <b>2015</b> , 137, 14887-904	6.4	295
319	Enhancing the Catalytic Activity of Hollandite Manganese Oxide by Supporting Sub-10 nm Ceria Particles. <b>2015</b> , 145, 1880-1884		7
318	Ag-embedded MnO nanorod: facile synthesis and oxygen reduction. <b>2015</b> , 17, 7646-7652		4
317	Efficient catalytic aerobic oxidation of thlorinated phenols with mixed-valent manganese oxide nanoparticles. <b>2015</b> , 90, 80-86		21
316	Highly reversible capacity at the surface of a lithium-rich manganese oxide: a model study using an epitaxial film system. <b>2015</b> , 51, 1673-6		27
315	Potassium-Based $\Box$ -Manganese Dioxide Nanofiber Binder-Free Self-Supporting Electrodes: A Design Strategy for High Energy Density Batteries. <b>2016</b> , 4, 1358-1368		17
314	The Origin of Oxygen Vacancies Controlling La2/3Sr1/3MnO3 Electronic and Magnetic Properties. <b>2016</b> , 3, 1500753		58
313	Cerium, manganese and cerium/manganese ceramic monolithic catalysts. Study of VOCs and PM removal. <b>2016</b> , 34, 675-682		35
312	Gold on Different Manganese Oxides: Ultra-Low-Temperature CO Oxidation over Colloidal Gold Supported on Bulk-MnO2 Nanomaterials. <i>Journal of the American Chemical Society</i> , <b>2016</b> , 138, 9572-80	6.4	73
311	A High Voltage Olivine Cathode for Application in Lithium-Ion Batteries. <b>2016</b> , 9, 223-30		28

310	Passivation Layer and Cathodic Redox Reactions in Sodium-Ion Batteries Probed by HAXPES. <b>2016</b> , 9, 97-108	53
309	Manganese oxide octahedral molecular sieve K-OMS-2 as catalyst in post plasma-catalysis for trichloroethylene degradation in humid air. <b>2016</b> , 314, 88-94	29
308	Birnessite-Type Manganese Oxide on Granular Activated Carbon for Formaldehyde Removal at Room Temperature. <i>Journal of Physical Chemistry C</i> , <b>2016</b> , 120, 24121-24129	60
307	CO oxidation over gold supported on Cs, Li and Ti-doped cryptomelane materials. <b>2016</b> , 480, 17-29	12
306	Crystallization design of MnO2via acid towards better oxygen reduction activity. <b>2016</b> , 18, 6895-6902	19
305	Determining the valence state of manganese ions in complex oxides La1 $\mbox{1}$ Ca x MnO3 (x = 0.5, 0.7, 0.85, and 0.9) based on Mn2p and Mn3s X-ray photoelectron spectra. <b>2016</b> , 80, 638-640	O
304	Superconductor to Mott insulator transition in YBa2Cu3O7/LaCaMnO3 heterostructures. <b>2016</b> , 6, 33184	7
303	Rational design of MnO@MnO hierarchical nanomaterials and their catalytic activities. 2016, 45, 18851-1885	8 18
302	EMnO-MnO Nanocomposite for Photochemical Water Oxidation: Active Structure Stabilized in the Interface. <b>2016</b> , 8, 27825-27831	45
301	Valence state of Mn in La1\(\mathbb{\text{S}}\)frxMnO3 probed by resonant Mn 3s-\(\mathbb{\text{g}}\)p x-ray emission spectroscopy. <b>2016</b> , 41, 341-346	
300	Hydrogenation of biomass-derived compounds containing a carbonyl group over a copper-based nanocatalyst: Insight into the origin and influence of surface oxygen vacancies. <b>2016</b> , 340, 184-195	75
299	Relationship between catalytic deactivation and physicochemical properties of LaMnO3 perovskite catalyst during catalytic oxidation of vinyl chloride. <b>2016</b> , 186, 173-183	68
298	Bi-template assisted synthesis of mesoporous manganese oxide nanostructures: Tuning properties for efficient CO oxidation. <b>2016</b> , 18, 5253-63	23
297	Active Mn species well dispersed on Ca2+ enriched apatite for total oxidation of toluene. <b>2016</b> , 184, 87-95	35
296	Multitechnique characterisation of 304L surface states oxidised at high temperature in steam and air atmospheres. <i>Applied Surface Science</i> , <b>2016</b> , 369, 510-519	11
295	XPS determination of Mn oxidation states in Mn (hydr)oxides. <i>Applied Surface Science</i> , <b>2016</b> , 366, 475-48 <b>6</b> . <sub>7</sub>	401
294	Catalytic oxidation of toluene over active MnO x catalyst prepared via an alkali-promoted redox precipitation method. <b>2016</b> , 118, 605-619	18
293	Effective recycling of manganese oxide cathodes for lithium based batteries. <b>2016</b> , 18, 3414-3421	44

292	Ba-doping effects on structural, magnetic and vibrational properties of disordered La2NiMnO6. <i>Journal of Alloys and Compounds</i> , <b>2016</b> , 663, 899-905	21
291	Effect of Mn substitution on the promoted formaldehyde oxidation over spinel ferrite: Catalyst characterization, performance and reaction mechanism. <b>2016</b> , 182, 476-484	109
<b>2</b> 90	Enhanced catalytic degradation of ciprofloxacin over Ce-doped OMS-2 microspheres. <b>2016</b> , 181, 561-569	92
289	Combination of non-thermal plasma and Pd/LaMnO3 for dilute trichloroethylene abatement.  Chemical Engineering Journal, 2016, 283, 668-675	37
288	Strain-Engineered Oxygen Vacancies in CaMnO Thin Films. <b>2017</b> , 17, 794-799	64
287	The effect of acid/alkali treatment on the catalytic combustion activity of manganese oxide octahedral molecular sieves. <b>2017</b> , 7, 3958-3965	21
286	Synthesis of manganese dioxide by homogeneous hydrolysis in the presence of melamine. <b>2017</b> , 62, 139-149	4
285	Enhanced Electrochemical Performance in Ni-Doped LiMn2O4-Based Composite Cathodes for Lithium-Ion Batteries. <b>2017</b> , 4, 1362-1371	12
284	Catalytic combustion of dimethyl ether over $\oplus$ -MnO 2 nanostructures with different morphologies. <i>Applied Surface Science</i> , <b>2017</b> , 409, 223-231	27
283	Catalytic properties of manganese oxide polyhedra with hollow and solid morphologies in toluene removal. <i>Applied Surface Science</i> , <b>2017</b> , 405, 20-28	64
282	Effect of temperature on the electrochemical synthesis of MnO 2 recycled from spent ZnMnO 2 alkaline batteries and application of recycled MnO 2 as electrochemical pseudocapacitors. <b>2017</b> , 196, 126-136	6
281	Electron structure, Raman Nacancylmodes and Griffiths-like phase of self-doped Pr1-xMnO3+ll manganites. <i>Journal of Alloys and Compounds</i> , <b>2017</b> , 722, 77-82	9
280	Pristine Surface Investigation of Li1.2Mn0.54Ni0.13Co0.13O2 towards Improving Capacity and Rate-capability for Lithium-ion Batteries. <b>2017</b> , 245, 118-127	7
279	Direct observation of enhanced water and carbon dioxide reactivity on multivalent metal oxides and their composites. <b>2017</b> , 10, 919-923	14
278	Cerium modified birnessite-type MnO2 for gaseous formaldehyde oxidation at low temperature. <b>2017</b> , 211, 212-221	176
277	A Simple and Green Procedure to Prepare Efficient Manganese Oxide Nanopowder for the Low Temperature Removal of Formaldehyde. <b>2017</b> , 9, 2366-2376	17
276	A novel LiCoPO4-coated coreShell structure for spinel LiNi0.5Mn1.5O4 as a high-performance cathode material for lithium-ion batteries. <i>Journal of Materials Chemistry A</i> , <b>2017</b> , 5, 996-1004	51
275	(La1\(\mathbb{R}\)Srx)0.98MnO3 perovskite with A-site deficiencies toward oxygen reduction reaction in aluminum-air batteries. <b>2017</b> , 342, 192-201	64

274	Giant Polarization Sustainability in Ultrathin Ferroelectric Films Stabilized by Charge Transfer. <b>2017</b> , 29, 1703543		35
273	Positive role of oxygen vacancy in electrochemical performance of CoMn 2 O 4 cathodes for Li-O 2 batteries. <b>2017</b> , 365, 134-147		62
272	A facile strategy to construct binder-free flexible carbonate composite anode at low temperature with high performances for lithium-ion batteries. <b>2017</b> , 246, 1004-1015		16
271	Enhanced Lithium Diffusion of Layered Lithium-Rich oxides with LixMn1.5Ni0.5O4 Nanoscale Surface Coating. <b>2017</b> , 247, 617-625		15
270	Synthesis of cryptomelane type ∃-MnO2 (KxMn8O16) cathode materials with tunable K+ content: the role of tunnel cation concentration on electrochemistry. <i>Journal of Materials Chemistry A</i> , <b>2017</b> , 5, 16914-16928	3	73
269	Defective and E-Disordered[Hortensia-like Layered MnOx as an Efficient Electrocatalyst for Water Oxidation at Neutral pH. <b>2017</b> , 7, 6311-6322		50
268	The relationship between surface open cells of ⊞-MnO2 and CO oxidation ability from a surface point of view. <i>Journal of Materials Chemistry A</i> , <b>2017</b> , 5, 20911-20921	3	31
267	Charge transfer effect for the La0.7Ca0.3MnO3/NiO heterostructure and novel interfacial ferromagnetism. <b>2017</b> , 138, 45-50		2
266	Tunnel Structured ⊞-MnO2with Different Tunnel Cations (H+, K+, Ag+) as Cathode Materials in Rechargeable Lithium Batteries: The Role of Tunnel Cation on Electrochemistry. <b>2017</b> , 164, A1983-A1990		26
265	Full microwave synthesis of advanced Li-rich manganese based cathode material for lithium ion batteries. <b>2017</b> , 337, 82-91		67
264	Rapid determination of the Mn average oxidation state of Mn oxides with a novel two-step colorimetric method. <b>2017</b> , 9, 103-109		26
263	Deconvolution of Composition and Crystallite Size of Silver Hollandite Nanorods: Influence on Electrochemistry. <b>2017</b> , 164, A3814-A3823		6
262	B-site ordering, magnetic and dielectric properties of hydrothermally synthesized Lu2NiMnO6. <i>Journal of Alloys and Compounds</i> , <b>2018</b> , 744, 395-403	·7	5
261	Fabrication of Na0.7MnO2/C composite cathode material by simple heat treatment for high-power na-ion batteries. <b>2018</b> , 14, 30-36		4
260	Hybridization of electronic states and magnetic properties of self-doped La1MnO3+ (0 Ix ID.15) perovskites: XANES study. <i>Journal of Magnetism and Magnetic Materials</i> , <b>2018</b> , 458, 134-136	.8	4
259	A cryogenic XPS study of Ce fixation on nanosized manganite and vernadite: Interfacial reactions and effects of fulvic acid complexation. <b>2018</b> , 483, 304-311		6
258	Structural and magnetic properties, magnetocaloric effect in (La 0.7 Pr 0.3 ) 0.8 Sr 0.2 Mn 0.9 Ti 0.1 O 3\(\mathrear\) [1 0.03, 0.02, \(\mathrear\) 0.03). Journal of Alloys and Compounds, <b>2018</b> , 751, 96-106	·7	7
257	Ethyl and butyl acetate oxidation over manganese oxides. <b>2018</b> , 39, 27-36		9

256	Cosputtered Calcium Manganese Oxide Electrodes for Water Oxidation. 2018, 57, 785-792	16
255	Valence state of cations in manganites Pr1-Ca MnO3 (0.3 🗷 🗓 .5) from X-ray diffraction and X-ray photoelectron spectroscopy. <i>Journal of Alloys and Compounds</i> , <b>2018</b> , 740, 132-142	9
254	Correlating Voltage Profile to Molecular Transformations in Ramsdellite MnO2 and Its Implication for Polymorph Engineering of Lithium Ion Battery Cathodes. <i>Journal of Physical Chemistry C</i> , <b>2018</b> , 122, 11689-11700	8
253	Electronic structure of the dilute magnetic semiconductor Ga1\( \text{M}\) MnxP from hard x-ray photoelectron spectroscopy and angle-resolved photoemission. <i>Physical Review B</i> , <b>2018</b> , 97,	10
252	Engineering Crystal Facet of ⊞-MnO2 Nanowire for Highly Efficient Catalytic Oxidation of Carcinogenic Airborne Formaldehyde. <b>2018</b> , 8, 3435-3446	257
251	Effect of Mn loading onto hydroxyapatite supported Mn catalysts for toluene removal: Contribution of PCA assisted ToF-SIMS. <b>2018</b> , 307, 41-47	8
250	Reaction of formaldehyde over birnessite catalyst: A combined XPS and ToF-SIMS study. <b>2018</b> , 223, 192-200	37
249	Aerobic Oxygenation of Alkylarenes over Ultrafine Transition-Metal-Containing Manganese-Based Oxides. <b>2018</b> , 10, 1096-1106	19
248	Monodisperse manganese oxide nanoparticles: Synthesis, characterization, and chemical reactivity. <b>2018</b> , 510, 272-279	22
247	Enhanced catalytic performance by oxygen vacancy and active interface originated from facile reduction of OMS-2. <i>Chemical Engineering Journal</i> , <b>2018</b> , 331, 626-635	66
246	Supported and unsupported manganese oxides for catalytic ammonia combustion. 2018, 105, 48-51	6
246	Supported and unsupported manganese oxides for catalytic ammonia combustion. <b>2018</b> , 105, 48-51  Effect of ball milling conditions on microstructure and lithium storage properties of LiNi0.5Mn1.5O4 as cathode for lithium-ion batteries. <b>2018</b> , 99, 436-443	6
,	Effect of ball milling conditions on microstructure and lithium storage properties of	
245	Effect of ball milling conditions on microstructure and lithium storage properties of LiNi0.5Mn1.5O4 as cathode for lithium-ion batteries. <b>2018</b> , 99, 436-443  Modified structural characteristics and enhanced electrochemical properties of oxygen-deficient	6
245 244	Effect of ball milling conditions on microstructure and lithium storage properties of LiNi0.5Mn1.5O4 as cathode for lithium-ion batteries. 2018, 99, 436-443  Modified structural characteristics and enhanced electrochemical properties of oxygen-deficient Li2MnO3-lbbtained from pristine Li2MnO3. 2018, 374, 134-141  A Nano-Architectured Metal-Oxide/Perovskite Hybrid Material as Electrocatalyst for the Oxygen	34
245 244 243	Effect of ball milling conditions on microstructure and lithium storage properties of LiNi0.5Mn1.5O4 as cathode for lithium-ion batteries. 2018, 99, 436-443  Modified structural characteristics and enhanced electrochemical properties of oxygen-deficient Li2MnO3-lbbtained from pristine Li2MnO3. 2018, 374, 134-141  A Nano-Architectured Metal-Oxide/Perovskite Hybrid Material as Electrocatalyst for the Oxygen Reduction Reaction in AluminumAir Batteries. 2018, 1, 6824-6833  Electronic structure of PrMnNiO from x-ray photoemission, absorption and density functional	6 34 10
245 244 243	Effect of ball milling conditions on microstructure and lithium storage properties of LiNi0.5Mn1.5O4 as cathode for lithium-ion batteries. 2018, 99, 436-443  Modified structural characteristics and enhanced electrochemical properties of oxygen-deficient Li2MnO3-lbbtained from pristine Li2MnO3. 2018, 374, 134-141  A Nano-Architectured Metal-Oxide/Perovskite Hybrid Material as Electrocatalyst for the Oxygen Reduction Reaction in Aluminum Batteries. 2018, 1, 6824-6833  Electronic structure of PrMnNiO from x-ray photoemission, absorption and density functional theory. 2018, 30, 435603  Photochemical Water Oxidation in a Buffered Tris(2,2'-bipyridyl)ruthenium-Persulfate System	6 34 10 3

238	Depth-resolved charge reconstruction at the LaNiO3/CaMnO3 interface. <i>Physical Review B</i> , <b>2018</b> , 98,	3	8
237	Investigation of nitrogen incorporation into manganese based copper diffusion barrier layers for future interconnect applications. <b>2018</b> , 13, 133-138		4
236	Transformation of birnessite into hollandite under the influence of silver cations in aqueous medium. <b>2018</b> , 268, 136-148		5
235	Mn-based mixed oxides for low temperature NOx adsorber applications. <b>2018</b> , 567, 90-101		16
234	Recycling application of waste LiMnO2 batteries as efficient catalysts based on electrochemical lithiation to improve catalytic activity. <b>2018</b> , 20, 4901-4910		32
233	Morphology Control Studies of MnTiO Nanostructures with Exposed {0001} Facets as a High-Performance Catalyst for Water Purification. <b>2018</b> , 10, 31631-31640		14
232	The art of balance: Engineering of structure defects and electrical conductivity of ⊞-MnO2 for oxygen reduction reaction. <b>2018</b> , 283, 459-466		38
231	Birnessite manganese oxide nanosheets assembled on Ni foam as high-performance pseudocapacitor electrodes: Electrochemical oxidation driven porous honeycomb architecture 6. formation. <i>Applied Surface Science</i> , <b>2018</b> , 458, 10-17	7	23
230	MnO2 nanoparticles anchored on carbon nanotubes with hybrid supercapacitor-battery behavior for ultrafast lithium storage. <b>2018</b> , 139, 145-155		58
229	Structural transformation, Griffiths phase and metal-insulator transition in polycrystalline Nd Sr NiMnO ( $x = 0, 0.2, 0.4, 0.5$ and 1) compound. <b>2018</b> , 30, 355401		3
228	Silver incorporated into cryptomelane-type Manganese oxide boosts the catalytic oxidation of benzene. <b>2018</b> , 239, 214-222		71
227	Selective Oxidation of Biomass-Derived Alcohols and Aromatic and Aliphatic Alcohols to Aldehydes with O/Air Using a RuO-Supported MnO Catalyst. <b>2018</b> , 3, 7944-7954		17
226	Macroscopic, theoretical simulation and spectroscopic investigation on the immobilization mechanisms of Ni(II) at cryptomelane/water interfaces. <b>2018</b> , 210, 392-400		3
225	A horizontal zinc-air battery with physically decoupled oxygen evolution/reduction reaction electrodes. <b>2018</b> , 393, 108-118		24
224	Partial Surface Oxidation of Manganese Oxides as an Effective Treatment To Improve Their Activity in Electrochemical Oxygen Reduction Reaction. <i>Journal of Physical Chemistry C</i> , <b>2018</b> , 122, 21366-21374 <sup>3-3</sup>	3	10
223	The effect of tungsten doping on the catalytic activity of ⊞-MnO2 nanomaterial for ozone decomposition under humid condition. <b>2018</b> , 562, 132-141		54
222	Electrochemical Oxidation of 5-Hydroxymethylfurfural to 2,5-Furandicarboxylic Acid (FDCA) in Acidic Media Enabling Spontaneous FDCA Separation. <b>2018</b> , 11, 2138-2145		83
221	Study of x-ray photo-emission spectroscopy and multiple metal to insulator transitions in an electron doped system of La1-xZrxMnO3 (x\mathbb{L}0.10, 0.20). <i>Journal of Alloys and Compounds</i> , <b>2019</b> , 770, 1049-1054	7	4

220	The promotional role of Nd on Mn/TiO2 catalyst for the low-temperature NH3-SCR of NOx. <b>2019</b> , 332, 49-58		25	
219	Modulating Oxygen Evolution Reactivity in MnO2 through Polymorphic Engineering. <i>Journal of Physical Chemistry C</i> , <b>2019</b> , 123, 22345-22357	3.8	18	
218	Low-valence or tetravalent cation doping of manganese oxide octahedral molecular sieve (K-OMS-2) materials for nitrogen oxide emission abatement. <b>2019</b> , 9, 4108-4117		13	
217	Reactive Grinding Synthesis of LaBO3 (B: Mn, Fe) Perovskite; Properties for Toluene Total Oxidation. <b>2019</b> , 9, 633		12	
216	Efficient catalytic removal of airborne ozone under ambient conditions over manganese oxides immobilized on carbon nanotubes. <b>2019</b> , 9, 4036-4046		28	
215	Solid-State Gelation for Nanostructured Perovskite Oxide Aerogels. <b>2019</b> , 31, 9422-9429		12	
214	Understanding charge compensation mechanisms in Na0.56Mg0.04Ni0.19Mn0.70O2. <b>2019</b> , 2,		10	
213	Structural and morphological alterations induced by cobalt substitution in LaMnO perovskites. <b>2019</b> , 556, 658-666		13	
212	Tuning Mn2+ additive in the aqueous electrolyte for enhanced cycling stability of birnessite electrodes. <b>2019</b> , 298, 678-684		8	
211	Influence of preparation temperature and acid treatment on the catalytic activity of MnO2. <b>2019</b> , 272, 173-181		15	
210	Surface and bulk charge distribution in manganese sulfide doped with lanthanide ions. <i>Applied Surface Science</i> , <b>2019</b> , 492, 209-218	6.7	5	
209	A facile one-pot hydrothermal synthesis as an efficient method to modulate the potassium content of cryptomelane and its effects on the redox and catalytic properties. <b>2019</b> , 40, 940-952		6	
208	Efficiency of manganese modified CTAB-templated ceria-zirconia catalysts in total CO oxidation. <i>Applied Surface Science</i> , <b>2019</b> , 485, 432-440	6.7	15	
207	Self-doped La1-xMnO3+[perovskites: Electron state hybridization and Raman modes. <b>2019</b> , 94, 41-44		7	
206	Microscopic Mechanisms of Local Interfacial Resistive Switching in LaMnO3+\(\textstyle{\pi}\)ACS Applied Electronic Materials, <b>2019</b> , 1, 675-683	4	10	
205	XPS on Nd0.6-Bi Sr0.4MnO3 nano powders. <i>Applied Surface Science</i> , <b>2019</b> , 487, 17-21	6.7	13	
204	Facile synthesis of Mn2.1V0.9O4/rGO: A novel high-rate anode material for lithium-ion batteries. <b>2019</b> , 426, 197-204		19	
203	Investigation of the self-discharge behaviors of the LiMn2O4 cathode at elevated temperatures: in situ X-ray diffraction analysis and a co-doping mitigation strategy. <i>Journal of Materials Chemistry A</i> , <b>2019</b> , 7, 13364-13371	13	23	

202	Improving the cycle life of cryptomelane type manganese dioxides in aqueous rechargeable zinc ion batteries: The effect of electrolyte concentration. <b>2019</b> , 305, 423-432		39
201	Three-dimensionally ordered macroporous K0.5MnCeOx/SiO2 catalysts: facile preparation and worthwhile catalytic performances for soot combustion. <b>2019</b> , 9, 1372-1386		16
200	Preparation of Ce?Mn Composite Oxides with Enhanced Catalytic Activity for Removal of Benzene through Oxalate Method. <b>2019</b> , 9,		9
199	Vanadium-doped MnO2 for efficient room-temperature catalytic decomposition of ozone in air. <i>Applied Surface Science</i> , <b>2019</b> , 484, 45-53	6.7	28
198	Temperature dependent transport properties and rectification in La0.7Sr0.3MnO3/La0.7Te0.3MnO3 pB junctions. <b>2019</b> , 12, 051013		2
197	Simultaneous catalytic elimination of formaldehyde and ozone over one-dimensional rod-like manganese dioxide at ambient temperature. <b>2019</b> , 94, 2305		3
196	Inherent thermal regeneration performance of different MnO crystallographic structures for mercury removal. <b>2019</b> , 374, 267-275		29
195	Fluorinated hexagonal 4H SrMnO3: a locally disordered manganite. <b>2019</b> , 7, 3560-3568		7
194	Enhanced catalytic ozonation towards oxalic acid degradation over novel copper doped manganese oxide octahedral molecular sieves nanorods. <b>2019</b> , 371, 42-52		31
193	Relevant electronic interactions related to the coordination chemistry of tetracyanometallates. An XPS study. <b>2019</b> , 43, 18384-18393		8
192	In Situ Hydrogen Uptake and NO Adsorption on Bifunctional Heterogeneous Pd/Mn/Ni for a Low Energy Path toward Selective Catalytic Reduction. <b>2019</b> , 4, 21340-21345		4
191	Fe-Doped ⊞-MnO nanorods for the catalytic removal of NO and chlorobenzene: the relationship between lattice distortion and catalytic redox properties. <b>2019</b> , 21, 25880-25888		14
190	Role of precursors mixing sequence on the properties of CoMnO cathode materials and their application in pseudocapacitor. <b>2019</b> , 9, 16852		7
189	Strain Manipulation of Magnetic Anisotropy in Room-Temperature Ferrimagnetic Quadruple Perovskite CeCu3Mn4O12. <i>ACS Applied Electronic Materials</i> , <b>2019</b> , 1, 2514-2521	4	2
188	High rate hybrid MnO2@CNT fabric anodes for Li-ion batteries: properties and a lithium storage mechanism study by in situ synchrotron X-ray scattering. <i>Journal of Materials Chemistry A</i> , <b>2019</b> , 7, 265	96 <sup>13</sup> 66	06 <sup>22</sup>
187	Tunable synthesis of LixMnO2 nanowires for aqueous Li-ion hybrid supercapacitor with high rate capability and ultra-long cycle life. <b>2019</b> , 413, 302-309		47
186	Influence of heavy metal sorption pathway on the structure of biogenic birnessite: Insight from the band structure and photostability. <b>2019</b> , 256, 116-134		14
185	Heat-Treatment-Assisted Molten-Salt Strategy to Enhance Electrochemical Performances of Li-Rich Assembled Microspheres by Tailoring Their Surface Features. <b>2019</b> , 25, 2003-2010		8

#### (2020-2019)

184	Synthesis of micron-sized LiNi0.5Mn1.5O4 single crystals through in situ microemulsion/coprecipitation and characterization of their electrochemical capabilities. <b>2019</b> , 343, 445-453	20
183	Thin Film All-solid-state Battery Using Li2MnO3 Epitaxial Film Electrode. <b>2019</b> , 48, 192-195	11
182	Synthesis of doped MnOx/diatomite composites for catalyzing ozone decomposition. <b>2019</b> , 45, 6966-6971	11
181	Native Vacancy Enhanced Oxygen Redox Reversibility and Structural Robustness. <b>2019</b> , 9, 1803087	50
180	Promoting diesel soot combustion efficiency by tailoring the shapes and crystal facets of nanoscale Mn3O4. <b>2019</b> , 242, 227-237	62
179	Tuning the fill percentage in the hydrothermal synthesis process to increase catalyst performance for ozone decomposition. <b>2020</b> , 87, 60-70	8
178	Effect of ball milling on the catalytic activity of cryptomelane for VOC oxidation. 2020, 41, 117-130	10
177	Mn promotion of rutile TiO2-RuO2 anodes for water oxidation in acidic media. <b>2020</b> , 261, 118225	31
176	Diatomite-supported birnessiteBype MnO2 catalytic oxidation of formaldehyde: Preparation, performance and mechanism. <i>Applied Surface Science</i> , <b>2020</b> , 502, 144201	27
175	Green Synthesis, Characterization and Test of MnO2 Nanoparticles as Catalyst in Biofuel Production from Grape Residue and Seeds Oil. <b>2020</b> , 11, 5003-5013	15
174	Enhanced cyclability and dynamic properties of P2-type Na0.59Co0.20Mn0.80O2 cathode by B-doping for sodium storage. <b>2020</b> , 529, 110582	
173	Evidence of ferromagnetic ordering at low temperatures in epitaxial TbMnO3 thin films grown by means of DC magnetron sputtering. <i>Journal of Magnetism and Magnetic Materials</i> , <b>2020</b> , 498, 166141	4
172	Self-assembly of MnO2 nanostructures into high purity three-dimensional framework for high efficiency formaldehyde mineralization. <b>2020</b> , 267, 118375	28
171	Controllable preparation of faceted Co3O4 nanocrystals@MnO2 nanowires shish-kebab structures with enhanced triethylamine sensing performance. <b>2020</b> , 304, 127358	22
170	MnOx-loaded Mesoporous Silica for the Catalytic Oxidation of Formaldehyde. Effect of the Melt Infiltration Conditions on the Activity (Stability Behavior. <b>2020</b> , 12, 1664-1675	3
169	The Promotional Effect of Copper in Catalytic Oxidation by Cu-Doped ⊞-MnO2 Nanorods. <i>Journal of Physical Chemistry C</i> , <b>2020</b> , 124, 701-708	10
168	Core-shell-like structured \(\frac{1}{2}\)-MnO2@CeO2 catalyst for selective catalytic reduction of NO: Promoted activity and SO2 tolerance. Chemical Engineering Journal, <b>2020</b> , 391, 123473	' 10
167	Electronic structure of CaMn1-Nb O3 (x=0.02, 0.04, 0.06 and 0.08) perovskites. Self-organization of terminal layers. <i>Journal of Alloys and Compounds</i> , <b>2020</b> , 820, 153106	2

166	Improving catalytic activity of layered lithium transition metal oxides for oxygen electrode in metal-air batteries. <b>2020</b> , 45, 1846-1856		12
165	Effect of A-site substitution by Ca or Sr on the structure and electrochemical performance of LaMnO3 perovskite. <b>2020</b> , 332, 135489		12
164	Stabilizing Li-rich layered cathode materials by nanolayer-confined crystal growth for Li-ion batteries. <b>2020</b> , 333, 135466		13
163	Proton Inserted Manganese Dioxides as a Reversible Cathode for Aqueous Zn-Ion Batteries. <b>2020</b> , 3, 319-327		23
162	Freezing-induced hierarchical porous manganese dioxide with excellent humidity tolerance for indoor formaldehyde removal. <b>2020</b> , 758, 137938		1
161	Ferromagnetic epitaxial Cr2O3 thin films grown on oxide substrates by Pulsed Laser Deposition. <i>Applied Surface Science</i> , <b>2020</b> , 534, 147638	6.7	O
160	Nanostructured Electrode Enabling Fast and Fully Reversible MnO2-to-Mn2+ Conversion in Mild Buffered Aqueous Electrolytes. <b>2020</b> , 3, 7610-7618		8
159	A Y(III)-based Metal-Organic Framework as a Carrier in Chemodynamic Therapy. <b>2020</b> , 59, 17276-17281		9
158	Laser photonic-reduction stamping for graphene-based micro-supercapacitors ultrafast fabrication. <b>2020</b> , 11, 6185		34
157	Surface modification of layer-tunnel hybrid Na0.6MnO2 cathode with open tunnel structure Na2Ti6O13. <i>Journal of Alloys and Compounds</i> , <b>2020</b> , 849, 156441	5.7	7
156	Harvesting the vibration energy of ⊞-MnO nanostructures for complete catalytic oxidation of carcinogenic airborne formaldehyde at ambient temperature. <b>2020</b> , 261, 127778		9
155	Recycling the Cathode Scrap of Spent Lithium-Ion Batteries as an Easily Recoverable Peroxymonosulfate Catalyst with Enhanced Catalytic Performance. <b>2020</b> , 8, 11337-11347		11
154	NaS Treatment and Coherent Interface Modification of the Li-Rich Cathode to Address Capacity and Voltage Decay. <b>2020</b> , 12, 42660-42668		12
153	Synthesis and Characterization of a Multication Doped Mn Spinel, LiNiCuFeMnO, as 5 V Positive Electrode Material. <b>2020</b> , 5, 22861-22873		7
152	Jahn-Teller Disproportionation Induced Exfoliation of Unit-Cell Scale ?-MnO. <b>2020</b> , 59, 22659-22666		9
151	Jahn Teller Disproportionation Induced Exfoliation of Unit-Cell Scale ?-MnO2. <b>2020</b> , 132, 22848-22855		1
150	Soot Combustion over Niobium-Doped Cryptomelane (K-OMS-2) NanorodsRedox State of Manganese and the Lattice Strain Control the Catalysts Performance. <b>2020</b> , 10, 1390		4
149	Enhancing the electrochemical performance of Li-rich cathode material by a flexible precursor treatment method. <b>2020</b> , 357, 115498		2

#### (2020-2020)

148	Difference of Oxidation Mechanism between Light C3🖸4 Alkane and Alkene over Mullite YMn2O5 OxideslCatalyst. <b>2020</b> , 10, 7269-7282		28
147	Acid Washing of MnOx-SBA-15 Composites as an Efficient Way to Improve Catalytic Properties in HCHO Total Oxidation. <b>2020</b> , 6, 1237-1244		2
146	Scalable synthesis of water-dispersible 2D manganese dioxide monosheets. <b>2020</b> , 32, 015301		5
145	The positive effect of Ca on cryptomelane-type octahedral molecular sieve (K-OMS-2) catalysts for chlorobenzene combustion. <b>2020</b> , 576, 496-504		7
144	Electrochemical Synthesis and Investigation of Stoichiometric, Phase-Pure CoSb2O6 and MnSb2O6 Electrodes for the Oxygen Evolution Reaction in Acidic Media. <b>2020</b> , 3, 5563-5571		11
143	Surface Conditions That Constrain Alkane Oxidation on Perovskites. <b>2020</b> , 10, 7007-7020		16
142	Complete Formaldehyde Removal over 3D Structured Na1.1Mn4O8@Mn5O8 Biphasic-Crystals. <b>2020</b> , 12, 3512-3522		5
141	Low-temperature synthesis of ultrasmall spinel MnxCo3-xO4 nanoparticles for efficient oxygen reduction. <b>2020</b> , 41, 1818-1825		4
140	Probing the Surface of La0.6Sr0.4MnO3 in Water Vapor by In Situ Photon-In/Photon-Out Spectroscopy. <i>Journal of Physical Chemistry C</i> , <b>2020</b> , 124, 7893-7902	3.8	4
139	Band alignment at non-polar AlN/MnS interface investigated by hard X-ray photoelectron spectroscopy. <b>2020</b> , 59, SIIG07		1
138	Catalytic activity of porous manganese oxides for benzene oxidation improved via citric acid solution combustion synthesis. <b>2020</b> , 98, 196-204		9
137	The electronic structure, surface properties, and NO decomposition of mechanochemically synthesised LaMnO. <b>2020</b> , 22, 18774-18787		2
136	Oxidation of diclofenac by birnessite: Identification of products and proposed transformation pathway. <b>2020</b> , 98, 169-178		4
135	Toward a Reversible Mn4+/Mn2+ Redox Reaction and Dendrite-Free Zn Anode in Near-Neutral Aqueous Zn/MnO2 Batteries via Salt Anion Chemistry. <b>2020</b> , 10, 1904163		98
134	The remarkable effect of alkali earth metal ion on the catalytic activity of OMS-2 for benzene oxidation. <b>2020</b> , 250, 126211		10
133	Double hysteresis loops and enhanced mechanical quality factor of Mn-doped 0.75PMN-0.25PT ceramics. <b>2020</b> , 46, 13324-13330		6
132	Improved magnetic performance of Co-doped La2NiMnO6 ceramics prepared at low temperature. <b>2020</b> , 40, 1909-1916		5
131	Molybdenum-Doped Manganese Oxide as a Highly Efficient and Economical Water Oxidation Catalyst. <b>2020</b> , 10, 2074-2087		41

130	Photovoltaic Lithium-ion Battery with Layer-Structured Li2MnIII0.2MnIV0.8O2.9 Thin Film Chemically Fabricated for Cathodic Active Material. <b>2020</b> , 13, 1486	2
129	Self-assembled ⊞-MnO2 urchin-like microspheres as a high-performance cathode for aqueous Zn-ion batteries. <b>2020</b> , 63, 1196-1204	18
128	The effects of morphology, microstructure and mixed-valent states of MnO2 on the oxygen evolution reaction activity in alkaline anion exchange membrane water electrolysis. <b>2020</b> , 461, 228131	21
127	Conversion Mechanisms of Selective Extraction of Lithium from Spent Lithium-Ion Batteries by Sulfation Roasting. <b>2020</b> , 12, 18482-18489	43
126	The controllable synthesis of substitutional and interstitial nitrogen-doped manganese dioxide: the effects of doping sites on enhancing the catalytic activity. <i>Journal of Materials Chemistry A</i> , <b>2020</b> , 8, 8383-839	6 <sup>26</sup>
125	Crystal engineering of TMPOx-coated LiNi0.5Mn1.5O4 cathodes for high-performance lithium-ion batteries. <b>2020</b> , 39, 127-136	19
124	Highly efficient multi-metal catalysts for carbon dioxide reduction prepared from atomically sequenced metal organic frameworks. <b>2021</b> , 14, 493-500	4
123	The Effect of Heat Treatment in Different Atmospheres on Tungsten-doped MnO2 for Ozone Decomposition. <b>2021</b> , 43, 195-206	2
122	Synergistic effect of bulk phase doping and layered-spinel structure formation on improving electrochemical performance of Li-Rich cathode material. <b>2021</b> , 47, 7700-7710	7
121	Promoting oxygen evolution of IrO2 in acid electrolyte by Mn. <b>2021</b> , 366, 137448	9
120	Influence of Chemical Composition and Domain Morphology of Li2MnO3 on Battery Properties. <b>2021</b> , 4, 493-503	1
119	Hydroxide ion dependent ⊞-MnO2 enhanced via oxygen vacancies as the negative electrode for high-performance supercapacitors. <i>Journal of Materials Chemistry A</i> , <b>2021</b> , 9, 2872-2887	7
118	MnD Covalency Governs the Intrinsic Activity of Co-Mn Spinel Oxides for Boosted Peroxymonosulfate Activation. <b>2021</b> , 133, 278-284	2
117	Mn-O Covalency Governs the Intrinsic Activity of Co-Mn Spinel Oxides for Boosted Peroxymonosulfate Activation. <b>2021</b> , 60, 274-280	86
116	Irregularly Shaped Mn2O3 Nanostructures with High Surface Area for Water Oxidation. 2021, 4, 396-405	3
115	Precious Metal-Free LaMnO Perovskite Catalyst with an Optimized Nanostructure for Aerobic C-H Bond Activation Reactions: Alkylarene Oxidation and Naphthol Dimerization. <b>2021</b> , 13, 5099-5110	7
114	Promoting the Reversible Oxygen Redox Reaction of Li-Excess Layered Cathode Materials with Surface Vanadium Cation Doping. <b>2021</b> , 8, 2003013	8
113	Reactions of the LiMnO Cathode in an All-Solid-State Thin-Film Battery during Cycling. <b>2021</b> , 13, 7650-7663	1

112	TM LDH Meets Birnessite: A 2D-2D Hybrid Catalyst with Long-Term Stability for Water Oxidation at Industrial Operating Conditions. <b>2021</b> , 60, 9699-9705		20
111	Photoenhanced performance of Cobalt-intercalated 2-D manganese oxide sheets for rechargeable zinc batteries. <b>2021</b> , 19, 100612		5
110	Mixed crystalline phases and catalytic performance of OMS-2 based nanocomposites for one-pot synthesis of quinazolines with O2 as an oxidant. <b>2021</b> , 504, 111499		1
109	TM LDH Meets Birnessite: A 2D-2D Hybrid Catalyst with Long-Term Stability for Water Oxidation at Industrial Operating Conditions. <b>2021</b> , 133, 9785-9791		2
108	Predominance of Subsurface and Bulk Oxygen Vacancies in Reduced Manganese Oxide. <i>Journal of Physical Chemistry C</i> , <b>2021</b> , 125, 7990-7998	.8	2
107	Redox cycling of manganese by Bacillus horikoshii biET1 via oxygen switch. <b>2021</b> , 375, 137963		2
106	Grain growth kinetics, microstructure and magnetic properties of mechanically activated Nd1\( \text{Nd1}\( \text{CaxMnO3}\) \( \text{Imanganites}. \( \text{Journal of Alloys and Compounds}, \text{2021}, 864, 158816 \)	·7	3
105	Atomic layer deposited nanolaminates of zirconium oxide and manganese oxide from manganese(III)acetylacetonate and ozone. <b>2021</b> , 32,		1
104	Evaluation of Manganese Oxide Octahedral Molecular Sieves for CO and C3H6 Oxidation at Diesel Exhaust Conditions. <b>2021</b> , 2,		О
103	Engineering High-Spin State Cobalt Cations in Spinel Zinc Cobalt Oxide for Spin Channel Propagation and Active Site Enhancement in Water Oxidation. <b>2021</b> , 133, 14657-14665		2
102	Engineering High-Spin State Cobalt Cations in Spinel Zinc Cobalt Oxide for Spin Channel Propagation and Active Site Enhancement in Water Oxidation. <b>2021</b> , 60, 14536-14544		27
101	Vitamin C-Assisted Synthesized MnfLo Oxides with Improved Oxygen Vacancy Concentration: Boosting Lattice Oxygen Activity for the Air-Oxidation of 5-(Hydroxymethyl)furfural. <b>2021</b> , 11, 7828-7844	ŀ	21
100	Engineering Manganese Defects in MnO for Catalytic Oxidation of Carcinogenic Formaldehyde. <b>2021</b> , 13, 29664-29675		2
99	High-performance adjustable manganese oxides hybrid nanostructure for supercapacitors. <b>2021</b> , 381, 138213		6
98	Effect of reduced local lattice disorder on the magnetic properties of B-site substituted La0.8Sr0.2MnO3. <i>Journal of Magnetism and Magnetic Materials</i> , <b>2021</b> , 529, 167893	.8	1
97	Encapsulate <code>H-MnO</code> nanofiber within graphene layer to tune surface electronic structure for efficient ozone decomposition. <b>2021</b> , 12, 4152		19
96	Rich bulk oxygen Vacancies-Engineered MnO2 with enhanced charge transfer kinetics for supercapacitor. <i>Chemical Engineering Journal</i> , <b>2021</b> , 417, 129186	4.7	25
95	Enhanced activity of Pd/⊞-MnO2 for electrocatalytic oxygen evolution reaction. <b>2021</b> , 46, 26976-26988		1

94	Post-Plasma Catalysis for Trichloroethylene Abatement with Ce-Doped Birnessite Downstream DC Corona Discharge Reactor. <b>2021</b> , 11, 946		
93	Novel cryptomelane nanosheets for the superior catalytic combustion of oxygenated volatile organic compounds. <b>2021</b> , 417, 126111		2
92	In-situ growth of cobalt manganate spinel nanodots on carbon black toward high-performance zinc-air battery: Dual functions of 3-aminopropyltriethoxysilane. <b>2022</b> , 608, 386-395		1
91	The role of Co substitution in the structural characteristics and magnetic properties of La2CoxNi1-xMnO6 epitaxial film. <i>Applied Surface Science</i> , <b>2021</b> , 561, 150102	6.7	1
90	Exploring a Co-Free, Li-Rich Layered Oxide with Low Content of Nickel as a Positive Electrode for Li-Ion Battery.		6
89	The Influence of the Chemical Potential on Defects and Function of Perovskites in Catalysis. <b>2021</b> , 9, 746229		
88	La1⊠SrxMnO3 Thin Films on Silicon Prepared by Magnetron Sputtering: Optimization of the Film Structure and Magnetic Properties by Postdeposition Annealing. 2100307		
87	Evaluation of Manganese Cubanoid Clusters for Water Oxidation Catalysis: From Well-Defined Molecular Coordination Complexes to Catalytically Active Amorphous Films. <b>2021</b> , 14, 4741-4751		1
86	Gd induced modifications in the magnetocaloric properties of dysprosium manganites. <i>Journal of Alloys and Compounds</i> , <b>2021</b> , 883, 160862	5.7	1
85	Significant enhancement of VOCs conversion by facile mechanochemistry coupled MnO2 modified fly ash: Mechanism and application. <i>Fuel</i> , <b>2021</b> , 304, 121443	7.1	2
84	Acid treated Ce modified birnessitelype MnO2 for ozone decomposition at low temperature: Effect of nitrogen containing co-pollutants and water. <i>Applied Surface Science</i> , <b>2022</b> , 571, 151240	6.7	0
83	Development of LnMnO perovskite on low temperature Hg removal 2022, 113, 141-151		O
82	Facile preparation of amorphous CenMnOx catalysts and their good catalytic performance for soot combustion. <i>Fuel</i> , <b>2022</b> , 307, 121803	7.1	2
81	Identifying the effect of fluorination on cation and anion redox activity in Mn based cation-disordered cathode. <b>2022</b> , 607, 1333-1342		1
80	Influence of the MnO2 Phase on Oxygen Evolution Reaction Performance for Low-Loading Iridium Electrocatalysts. <b>2021</b> , 8, 418-424		2
79	Manipulating Surface Termination of Perovskite Manganate for Oxygen Activation. <b>2021</b> , 31, 2006439		7
78	NiMnOx/TiN/CC electrode with a branchleaf structure: a novel approach to improve the performance of supercapacitors with high mass loading of amorphous metal oxides. <i>Journal of Materials Chemistry A</i> ,	13	3
77	Structural modulation in potassium birnessite single crystals. <b>2021</b> , 9, 1370-1377		2

76	Sodium Rivals Silver as Single-Atom Active Centers for Catalyzing Abatement of Formaldehyde. <i>Environmental Science &amp; Environmental Science &amp; Environm</i>	10.3	42
75	Self-standing LiMnNiO/graphene membrane as a binder-free cathode for Li-ion batteries <b>2018</b> , 8, 3976	9-397	76
74	Tuning electronic reconstructions at the cuprate-manganite interface. <b>2019</b> , 3,		3
73	Facile coating of MnO2 nanoparticles onto polymer fibers via friction-heating adhesion for efficient formaldehyde removal. <i>Chemical Engineering Journal</i> , <b>2022</b> , 430, 132954	14.7	3
72	In Situ Raman Spectroscopic Study of Species in Co-MnCeOx Catalysts under COPrOx Reaction Conditions.		
71	Electroresistance effect in oxygen-deficient LaBaMnO thin films. <b>2020</b> , 32, 425703		1
70	High-throughput design of NaBeMnD cathodes for Na-ion batteries. <i>Journal of Materials Chemistry A</i> ,	13	4
69	Facet control of manganese oxides with diverse redox abilities and acidities for catalytically removing hazardous 1,2-dichloroethane.		
68	Unraveling the Resistive Switching Mechanisms in LaMnO3+EBased Memristive Devices by Operando Hard X-ray Photoemission Measurements. <i>ACS Applied Electronic Materials</i> ,	4	1
67	Facet selectively exposed ⊞-MnO2 for complete photocatalytic oxidation of carcinogenic HCHO at ambient temperature. <i>Chemical Engineering Journal</i> , <b>2021</b> , 431, 133737	14.7	4
66	A Controllable Dual Interface Engineering Concept for Rational Design of Efficient Bifunctional Electrocatalyst for Zinc-Air Batteries. <b>2021</b> , e2105604		O
65	MnO2 nanoarray with oxygen vacancies: An efficient catalyst for NO electroreduction to NH3 at ambient conditions. <b>2021</b> , 22, 100586		18
64	High surface area MnO2 nanomaterials synthesized by selective cation dissolution for efficient water oxidation.		1
63	Application of rock-salt-type CoMn oxides for alkaline polymer electrolyte fuel cells. <b>2022</b> , 520, 230868		O
62	Emergent phenomena at oxide interfaces studied with standing-wave photoelectron spectroscopy. <b>2022</b> , 40, 020801		
61	Self-templated formation of hierarchical hollow EMnO2 microspheres with enhanced oxygen reduction activities. <b>2022</b> , 637, 128228		2
60	Mapping the magnetic state as a function of antisite disorder in Sm2NiMnO6 double perovskite thin films. <i>Physical Review B</i> , <b>2022</b> , 105,	3.3	1
59	Manipulating magnetic and magnetoresistive properties by oxygen vacancy complexes in GCMO thin films <b>2022</b> ,		

58	Promotion of Low-Temperature Oxidation of Propane through Introduction of Ce into Mullite Oxide YMn O <b>2022</b> , 87, e202100455		1
57	Electrochromic 2,5-Dihydroxyterephthalic Acid Linker in Metal©rganic Frameworks. 2100219		
56	Microwave Stimulation of Energetic Al-Based Nanoparticle Composites for Ignition Modulation.		1
55	Oxidative Decomposition with Peg-Mno2 Catalyst for Removal of Formaldehyde: Chemical Aspects on Hcho Oxidation Mechanism. <i>SSRN Electronic Journal</i> ,	1	
54	Ionic Liquid Gating Control of Oxygen Vacancies in the La0.8Ba0.2MnO3 Ultrathin Films. <b>2022</b> , 11, 027	002	
53	Enhanced Catalytic Ozonation for Eliminating CHSH Stable and Circular Electronic Metal-Support Interactions of Si-O-Mn Bonds with Low Mn Loading <i>Environmental Science &amp; Camp; Technology</i> , <b>2022</b> ,	10.3	3
52	Effects of Surface Polarity on the Structure and Magnetic Properties of Epitaxial h-YMnO3 Thin Films Grown on MgO Substrates. <i>ACS Applied Electronic Materials</i> ,	4	1
51	The positive role of the single crystal morphology in improving the electrochemical performance of Li-rich cathode materials. <i>Journal of Alloys and Compounds</i> , <b>2022</b> , 905, 164204	5.7	3
50	Reduced graphene oxide as a charge reservoir of manganese oxide: Interfacial interaction promotes charge storage property of MnO -based micro-supercapacitors. <i>Chemical Engineering Journal</i> , <b>2022</b> , 439, 135569	14.7	
49	Constructing MnO2 alpha/amorphous heterophase junction by mechanochemically induced phase transformation for formaldehyde oxidation. <i>Applied Surface Science</i> , <b>2022</b> , 589, 152855	6.7	1
48	Reaction Mechanism of LiMnO Electrodes in an All-Solid-State Thin-Film Battery Analyzed by Operando Hard X-ray Photoelectron Spectroscopy <i>Journal of the American Chemical Society</i> , <b>2021</b> ,	16.4	3
47	One step citric acid-assisted synthesis of Mn-Ce mixed oxides and their application to diesel soot combustion. <i>Fuel</i> , <b>2022</b> , 322, 124201	7.1	1
46	Lattice Expansion and Electronic Reconfiguration of Mncu Oxide Catalysts for Enhanced Transfer Hydrogenation of Levulinate. <i>SSRN Electronic Journal</i> ,	1	
45	Ozone Decomposition below Room Temperature Using Mn-based Mullite YMn2O5. <i>Environmental Science</i> & amp; Technology,	10.3	1
44	Two-Step Thermochemical CO2 Splitting Using Partially-Substituted Perovskite Oxides of La0.7Sr0.3Mn0.9X0.1O3 for Solar Fuel Production. <i>Frontiers in Energy Research</i> , 10,	3.8	0
43	Re-entrant Spin Glass and Magnetocaloric Effect in Frustrated Double Perovskite Ho2CoMnO6 Flat Nanorod. <i>Journal of Magnetism and Magnetic Materials</i> , <b>2022</b> , 559, 169537	2.8	1
42	Oxidative decomposition with PEG-MnO2 catalyst for removal of formaldehyde: Chemical aspects on HCHO oxidation mechanism. <i>Applied Surface Science</i> , <b>2022</b> , 598, 153773	6.7	0
41	Tunable Control of the Structural Features and Related Physical Properties of MnxFe3IIO4 Nanoparticles: Implication on Their Heating Performance by Magnetic Hyperthermia. <i>Journal of Physical Chemistry C</i> , <b>2022</b> , 126, 10110-10128	3.8	O

40	Experimental correlation of Mn3+ cation defects and electrocatalytic activity of $\oplus$ -MnO2 $\oplus$ n X-ray photoelectron spectroscopy study. <i>Journal of Materials Chemistry A</i> ,	0
39	Stable Colloid-in-acid Electrolytes for Long Life Proton Batteries. <i>Nano Energy</i> , <b>2022</b> , 107642 17.1	O
38	Aqueous proton battery stably operates in mild electrolyte and low-temperature conditions. <b>2022</b> , 10, 17288-17296	1
37	Selective dissolution to synthesize densely populated Pt single atom catalyst.	
36	Low-Temperature Hydrogenation of Methyl Acetate to Ethanol over a Manganese-Modified Cu/SiO2 Catalyst. <b>2022</b> , 61, 11718-11726	1
35	Reaction gas-induced partial exsolution of Pd from PdCeMnO for methane combustion. <b>2023</b> , 451, 138937	O
34	Dynamic evolution of structureEctivity of anode on lead release and overpotential change in zinc electrowinning. <b>2023</b> , 451, 138944	2
33	Mn-doped Co3O4 for acid, neutral and alkaline electrocatalytic oxygen evolution reaction. <b>2022</b> , 12, 26846-26858	1
32	A green process for recycling and synthesis of cathode materials LiMn2O4 from spent lithium-ion batteries using citric acid. <b>2022</b> , 12, 23683-23691	3
31	Utilization of Ag ions to improve room-temperature TCR of La0.85-Sr0.15Ag MnO3 polycrystalline ceramics. <b>2022</b> ,	Ο
30	Lattice Expansion and Electronic Reconfiguration of MnCu Oxide Catalysts for Enhanced Transfer Hydrogenation of Levulinate.	О
29	Effect of vinylene carbonate on SEI formation on LiMn2O4 in carbonate-based electrolytes. <b>2022</b> , 24, 25611-25619	1
28	Effect of Cu Substitution in P?2- and P2-Type Sodium Manganese-Based Oxides. 2022, 5, 12999-13010	O
27	Interdigital MnO 2 / PEDOT Alternating Stacked Microelectrodes for High-Performance On-Chip Microsupercapacitor and Humidity Sensing.	Ο
26	Room-temperature catalytic removal of indoor trace hexanal by weakly crystallized MnO2 ultrafine nanowires. <b>2022</b> , 226, 109701	1
25	Superior La0.67K0.33-Sr MnO3 films with room-temperature TCR prepared by spin coating method. <b>2023</b> , 610, 155589	Ο
24	Sulfuretted Li- and Mn-Rich Cathode Material with Epitaxial Spinel Stabilizer for Ultra-Long Cycle Li-Ion Battery. <b>2022</b> , 140398	0
23	Promoted catalytic performance of Ag-Mn bimetal catalysts synthesized through reduction route. <b>2022</b> ,	O

22	Defects and Surface Chemistry of Novel PH-Tunable NiO-Mn3O4⊞IMnxNi1-xO Heterostructured Nanocrystals as Determined Using X-ray Photoemission Spectroscopy.	О
21	In-situ investigation on the oxygen vacancy-driven topotactic phase transition in charge-orbital ordered Nd0.5Sr0.5MnO3 films. <b>2023</b> , 245, 118616	O
20	Facile Preparation of High Performance Low Concentration HCHO Degradation Catalyst from Waste Li-MnO2 Batteries.	O
19	Two-Dimensional Bimetallic Hydroxide Nanostructures for Catalyzing Low-Temperature Aerobic CH Bond Activation in Alkylarene and Alcohol Partial Oxidation. <b>2022</b> , 5, 18855-18870	O
18	Facile synthesis of single-crystalline MnO2 nanowire arrays with high photothermal catalytic activity.	O
17	Electron transfer enhancing the Mn(II)/Mn(III) cycle in MnO/CN towards catalytic ozonation of atrazine via a synergistic effect between MnO and CN. <b>2023</b> , 230, 119574	O
16	Enhanced Li storage properties of nickel oxalate microtubes with manganese doping and graphene oxide for lithium-ion batteries. <b>2023</b> , 940, 168808	O
15	Electrochemical in-situ generation of Ni-Mn MOF nanomaterials as anode materials for lithium-ion batteries. <b>2023</b> , 942, 168926	O
14	Mesoporous CeOx/MnOx catalyst derived from Mn-BTC for ozone catalytic decomposition. <b>2023</b> , 653, 119080	1
13	Effecting pattern study of SO2 on Hg0 removal over ⊞-MnO2 in-situ supported magnetic composite. <b>2023</b> , 450, 131088	O
12	Effect of cation vacancies in nonstoichiometric (LaMn)1-O3 on oxygen reduction reaction catalysis. <b>2023</b> , 946, 169398	O
11	Enhancing the performance and mechanical stability of 2D-based hybrid micro-supercapacitors using dendritic-gold as framework layer. <b>2023</b> , 453, 142346	O
10	Enhanced electrochemical performance of MnO2 by high oxidation state vanadium(V) doping. <b>2023</b> , 946, 169386	O
9	Facile synthesis of EMnO2 via ozone oxidation for enhanced performance of toluene oxidation. <b>2023</b> , 38, 102858	O
8	A Gradient Doping Strategy toward Superior Electrochemical Performance for Li-Rich Mn-Based Cathode Materials. 2207797	O
7	Amorphous K-Buserite Microspheres for High-Performance Aqueous Zn-Ion Batteries and Hybrid Supercapacitors. 2207329	O
6	MnOOH-Catalyzed Autoxidation of Glutathione for Reactive Oxygen Species Production and Nanocatalytic Tumor Innate Immunotherapy. <b>2023</b> , 145, 5803-5815	O
5	Exceptional Ozone Decomposition over EMnO2/AC under an Entire Humidity Environment.	O

#### CITATION REPORT

4	Substitutional effect of Mg 2+ on structural and magnetic properties of La 2 Mg x Ni 1-x MnO 6 double-perovskite thin films.	O
3	Molten salts synthesis of Li1.1Mn0.55Ni0.3Co0.05O2 oxide cathode material for lithium-ion batteries. <b>2023</b> , 58, 6151-6163	O
2	CeO2/ $\!$	O
1	Modulating the Proton-Conducting Lanes in Spinel ZnMn 2 O 4 through Off-Stoichiometry.	О